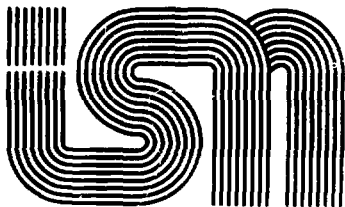


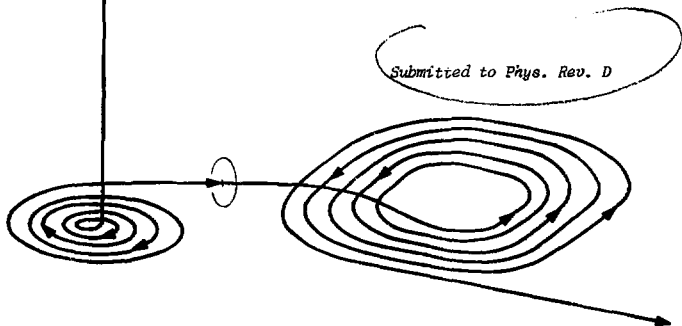
FR 8901011



SEARCH FOR DIQUARK CLUSTERING IN BARYONS

S. Fleck, B. Silvestre-Brac, J.M. Richard

Submitted to Phys. Rev. D



Search for diquark clustering in baryons

S. Fleck, B. Silvestre-Brac, and J.M. Richard

Institut des Sciences Nucléaires
53, avenue des Martyrs
F-38046 Grenoble Cedex

Abstract

In the framework of the non-relativistic quark model, we examine to which extent baryons consist of a quark bound to a localized cluster of two quarks simulating a diquark. We consider ground states and orbital excitations for various flavour combinations. A striking clustering shows up sometimes especially for the leading Regge trajectory of the nucleon and single flavoured baryons or for the ground state of baryons bearing two heavy flavours. This is, however, far from being a general pattern and there are clear differences between the three-quark description of baryons and the quark-diquark model.

I Introduction

Diquarks are almost as old as quarks. The notion of diquark was already suggested by Gell-Mann in his pioneering papers on quarks¹, and, since that time, there is every year an abundant literature on diquarks. The concept of diquark is, however, discussed from rather different points of view and a minimum clarification is needed before presenting our contribution.

In some theories of the fundamental structures, the diquark emerges from the very beginning as necessary for the internal consistency. This is the case for instance in the so-called topological bootstrap of Chew *et al.*². In such extreme approaches, the baryons are described as quark-antiquark bound states and the diquarks are either postulated as fundamental constituents on the same footing as quarks or built out of two quarks by *ad-hoc* short range forces.

In a more empirical approach, one does not postulate such new forces, but one assumes for simplicity that the baryons wave-function consists of a quark orbiting around a set of two-quarks whose clustering is due to the "ordinary" interquark potential only. For instance, in ref. 3, the baryon binding energy is estimated in two steps, first by computing the mass of a cluster D out of two quarks, and then by solving the two-body (D-q) problem. A good fit was obtained, but no comparison was attempted with the exact solution of the original three-body problem.

Our study is closer in spirit to the point of view adopted by Basdevant and Boukaraa⁴ and A.Martin⁵. In ref 4, a semi-relativistic calculation of low lying baryons was first done, using an extension of the hyperspherical formalism⁶. Then a comparison was shown with the two-step calculation, where the diquark D is built out of two-quarks and the baryon computed as a q-D system, generally in rather good agreement with the three-body binding energy. In ref 5, a semi-classical calculation shows that with a two-body or three-body linear confinement, associated with non-relativistic or relativistic kinematics, the states of high angular momentum lying on the leading Regge trajectory consist of a quark well separated from the two others, which form a localized cluster. This explains why meson and baryon Regge trajectories have the same slope.

The aim of the present paper is to study systematically this dynamical clustering inside baryons. First, we compare the mass spectrum obtained from the whole three-body hamiltonian to an approximate calculation where the baryon is made of a quark and a diquark. We also examine carefully the distribution of the interquark distances inside baryon wave-functions obtained from an accurate three body calculation. The non-relativistic prototype presented here allows one to discuss the various factors which can act in favour or against the formation of diquarks :

- i) asymmetry of the system. In a (QQq) baryon with double charm or beauty, the two heavy quarks experience less kinetic energy than the light one, and tend to stay close to each other.
- ii) angular momentum effect. One may be afraid that, if a baryon has a high spin, each pair of quarks should carry part of the angular momentum and, due to centrifugal repulsion, cannot form a diquark. The result of ref. 5 suggests, however, that one quark takes care of the whole angular momentum whereas the two others form a diquark.
- iii) spin-effect. The quark-quark potential contains a spin-spin component which is short ranged and favours the formation of a diquark with spin 0.
- iv) Pauli principle. Such a spin 0 diquark is forbidden for identical quarks which should arrange themselves in a spin triplet state for which the chromomagnetic forces are repulsive.

Each of these effects will be analyzed in detail. The asymmetry is studied by considering various flavour combinations $(q_1 q_2 q_3) = (qqq)$, (qqQ) or (qQQ) of light and heavy quarks, for which we examine all possible $(q_i q_j)$ diquarks. In each case, the role of the angular momentum L is analyzed by considering states with $L = 0$ and $L = 8$. Spin effects are exhibited by switching on

and off the spin dependent term of the potential. Comparing the (uuq) with the (udq) cases illustrates the constraints due to the Pauli principle.

The paper is organized as follows. The models and the relevant observables are defined in section II. The nucleon system (qqq) is analyzed in detail in section III, while the asymmetric configurations (qqQ) and (qQQ) are considered in sections IV and V. Our conclusions are drawn in the last section. Part of this work was already presented^{7,8} and additional details will be provided elsewhere⁹.

II The models

1. The potentials

We choose a simple constituent quark picture of baryons, ignoring relativistic corrections, although they are certainly important for light quarks, especially to get a linear Regge behaviour out of a linearly rising potential. Hopefully, the qualitative conclusions, concerning the presence or absence of clustering are not affected by the non-relativistic approximation.

In the following, we shall adopt two different two-body potentials, which are representative of the various models commonly used in the literature. The first one is the familiar "coulomb-plus-linear"¹⁰

$$V_{ij}^c = \frac{1}{2} \left(-\frac{a}{r_{ij}} + b r_{ij} + d \right) \quad (1)$$

which is supported by lattice calculations and which was extensively used for hadron spectroscopy.

The second one is the power law potential

$$V_{ij}^c = \frac{1}{2} (A + B r_{ij}^\beta) \quad (2)$$

which has been proposed by A. Martin¹¹ for mesons and extended with some success to baryon spectroscopy¹².

These potentials have to be supplemented by an hyperfine interaction of Breit-Fermi type

$$V_{ij}^{ss} = \frac{C}{2} \frac{\vec{\sigma}_i \cdot \vec{\sigma}_j}{m_i m_j} \delta(\vec{r}_{ij}) \quad (3)$$

If one treats the spin interactions non perturbatively, it is necessary to smear out the contact term (3), to avoid any collapse. One could use, for instance, the Yukawa form :

$$V_{ij}^{ss} = \frac{C}{2} \frac{\vec{\sigma}_i \cdot \vec{\sigma}_j}{m_i m_j} \frac{e^{-\Lambda r_{ij}}}{r_{ij}} \quad (4)$$

In the above formulae, m_i denotes the constituent quark mass. The 1/2 factor in front of the potentials is reminiscent from the rule $V_{qq} = 1/2 V_{q\bar{q}}$ which is often used to relate the quark potentials inside mesons and baryons¹².

We use the potential corresponding to (1) + (4) as proposed by Bhaduri *et al*¹³ with the parameters

$$a = 0.5203; b = 0.1857 \text{ GeV}^2; d = -0.9135 \text{ GeV}; \Lambda = 0.4341 \text{ GeV}; C = 0.0981 \text{ GeV}^2$$

$$m_q = 0.337 \text{ GeV}; m_s = 0.600 \text{ GeV}; m_c = 1.870 \text{ GeV}; m_b = 5.259 \text{ GeV}$$

A successful description of hadron spectroscopy has been achieved with this potential or with some improved versions elaborated by Ono *et al*¹⁴ or others. A purely linear potential is of particular interest to study the leading Regge trajectory and test the semi-classical result of Martin⁵. We adopt in that case the linear part of Bhaduri's potential and force the rest of the potential to vanishing values. For the potential (2), we adopt the parameters of ref. 12, namely :

$$\alpha = 0.1, A = -8.337, B = 6.9923$$

$$m_q = 0.300 \text{ GeV}; m_s = 0.600 \text{ GeV}; m_c = 1.895 \text{ GeV}; m_b = 5.255 \text{ GeV}$$

In the investigations presented in the next sections, both potentials have been used, with in general very similar results. This is why we will display only the density distributions corresponding to the coulomb-plus-linear potential.

2. The quark-diquark approximation

For a given flavour configuration ($q_1 q_2 q_3$), we assume *a priori* a diquark structure and approximate the exact three-body problem corresponding to the hamiltonian

$$H = \sum_{i=1}^3 \left(m_i + \frac{p_i^2}{2m_i} \right) + \sum_{i < j} V(r_{ij}) \quad (5)$$

by two successive two-body problems. First a diquark is built out of the quarks q_2 and q_3 , in s-wave and colour $\bar{3}$. If $q_2 = q_3$, the diquark is forced to be in a spin $\sigma = 1$ state as required by the Pauli principle, while non identical quarks give rise to a $\sigma = 0$ diquark which is more favoured energetically. More precisely, the diquark mass m_D is computed as the ground state of the two-body hamiltonian.

$$H_{23} = m_2 + m_3 + \frac{p_2^2}{2m_2} + \frac{p_3^2}{2m_3} + V(r_{23}) \quad (6)$$

The diquark is now considered as a point-like object and the approximate baryon mass is obtained from the hamiltonian

$$H_{qD} = m_1 + m_D + \frac{p_1^2}{2m_1} + \frac{p_D^2}{2m_D} + 2 V(r_{1D}) \quad (7)$$

The potential energy $2 V(r_{1D})$ is deduced from $V(r_{12}) + V(r_{13})$ in the limit $r_{12} = r_{13} = r_{1D}$. It is equal to the potential of a $q\bar{q}$ system. Spin 1/2 baryons are calculated in this approximation, with either angular momentum $L = 0$ or $L > 0$. In the later case, the angular momentum is carried by the quark motion around the diquark. Similar calculations are also performed with the ($q_2 q_3$) diquark replaced by ($q_1 q_2$) or ($q_1 q_3$).

Note that this approximation to the three-body problem might be not variational. Let us consider, indeed, the case of an harmonic oscillator potential $V = \frac{2}{3} r^2$, with $m_1 = m$ and $m_2=m_3=M$. Introducing the usual Jacobi coordinates $\vec{\rho} = \vec{r}_2 - \vec{r}_3$ and $\vec{\lambda} = (\vec{r}_2 + \vec{r}_3 - 2\vec{r}_1) / \sqrt{3}$ and the reduced mass μ given by $\mu^{-1} = \frac{1}{3} M^{-1} + \frac{2}{3} m^{-1}$, results into the hamiltonian

$$H = \frac{p_{\rho}^2}{M} + \frac{p_{\lambda}^2}{\mu} + \vec{\rho}^2 + \vec{\lambda}^2 \quad (8)$$

whose lowest eigen energy is $E_0 = 3 M^{-1/2} + 3 \mu^{-1/2}$.

On the other hand, the quark-diquark approximation gives a diquark mass $m_D = 2M + 3\sqrt{\frac{2}{3M}}$ and a baryon energy $E_D = 3\sqrt{\frac{2}{3M}} + 3\tilde{\mu}^{-1/2}$, where $\tilde{\mu}^{-1} = \frac{2}{3}(m^{-1} + m_D^{-1})$. Clearly $E_D < E_0$. First, the reduced mass μ has been increased to $\tilde{\mu}$, resulting into a decrease of the kinetic energy. Also, the potential energy $\vec{\rho}^2 + \vec{\lambda}^2$ has been decreased to $2/3 \vec{\rho}^2 + \vec{\lambda}^2$ by neglecting the diquark structure ($\vec{r}_{12} = \vec{r}_{13} = \vec{r}_{1D}$). Nothing can be said when the potential has negative powers as in the coulomb case, or when spin forces are present.

3. Scrutinizing the wave-function

The quark-diquark approximation of the previous section is tested only on its results for mass calculations, so even a good agreement with exact three-body energies would not prove that quarks do actually cluster. This is why we also calculate without approximation the three-quark wave-function and look whether it contains any diquark structure. This calculation is achieved by expanding the three-body wave-function $|\Psi\rangle$ on an harmonic oscillator basis

$$|\Psi_L\rangle = C \sum_{\sigma, n, l, m, k} d_{\sigma n l m k} |\chi_{\sigma}\rangle |[\phi_{nl}(\vec{\rho}) \phi_{mk}(\vec{\lambda})]_L\rangle \quad (8)$$

Here C denotes the colour-singlet wave-function, which is antisymmetric. For baryons with total spin $S = 1/2$, there are two possibilities of spin coupling for the pair (2-3), $\sigma = 0$ or 1, and thus two basic spin functions $|\chi_{\sigma}\rangle = |1/2(1/2, 1/2)_{\sigma}\rangle_{S=1/2}$. The spatial wave-function is expanded on harmonic oscillator basis $|\phi_{nl}\rangle$ for both relative Jacobi coordinates $\vec{\rho}$ and $\vec{\lambda}$ given by

$$\begin{cases} \vec{\rho} = \left(\frac{2m_2m_3}{m_2+m_3}\right)^{1/2} (\vec{r}_2 - \vec{r}_3) \\ \vec{\lambda} = \left(\frac{2m_1(m_2+m_3)}{m_1+m_2+m_3}\right)^{1/2} \left(\frac{m_2\vec{r}_2 + m_3\vec{r}_3}{m_2+m_3} - \vec{r}_1\right) \end{cases} \quad (9)$$

The two oscillators are coupled to a total angular momentum L which is conserved here since tensor and spin-orbit forces are neglected. This way of solving the Schrödinger equation has been described elsewhere¹⁵ in more detail. The total number of quanta $N = 2n + l + 2m + k$ is varied to check the convergence of the method. In practice, calculations performed in a basis with $N \leq 8$

turn out to be sufficiently accurate for our purpose. This means that we include 70 basis states for $L = 0$ and 18 basis states for $L = 8$. In the case of identical quarks, these numbers can be divided by two.

We define the one-body density $f_{\sigma}(\lambda)$

$$f_{\sigma}(\lambda) = \langle \Psi | P_{\sigma} \delta(\vec{\lambda} - \lambda) | \Psi \rangle = \int |P_{\sigma} \Psi(\vec{\rho}, \vec{\lambda})|^2 d\vec{\rho} \lambda^2 d\Omega_{\lambda} \quad (10)$$

with the normalization :

$$\sum_{\sigma} \int f_{\sigma}(\lambda) d\lambda = 1 \quad (11)$$

Here P_{σ} is the projector that forces particles 2 and 3 to be coupled to a spin $\sigma = 0$ or 1. Thus the function $f_{\sigma}(\lambda)$ represents the probability density to find the particles 2 and 3 coupled to spin σ and particle 1 at a distance λ from the centre-of-mass of the pair (2-3). We also define D as the value of λ which makes $\sum_{\sigma} f_{\sigma}(\lambda)$ maximum, i.e. the most probable distance between particle 1 and the pair (2-3).

We similarly define a two-body density $g_{\sigma}(\rho)$, by changing $\vec{\lambda}$ into $\vec{\rho}$ in the above formulae. The function $g_{\sigma}(\rho)$ represents the probability density to find particles 2 and 3 coupled to spin σ and at a distance ρ from each other. We call R the value of ρ which maximizes $\sum_{\sigma} g_{\sigma}(\rho)$, i.e. the most probable separation distance between quarks 2 and 3. If the density distributions $f_{\sigma}(\lambda)$ and $g_{\sigma}(\rho)$ are peaked such that $R \ll D$, this gives evidence for a (q_2q_3) diquark, as illustrated in fig. (1.a). On the other hand, mean values such as $R \equiv D$ could reveal either the absence of diquark, as in fig. (1.b) or a (q_1q_2) or (q_1q_3) clustering as in fig. (1.c). To look for (q_1q_2) or (q_1q_3) clustering with the actual choice (9) of Jacobi coordinates, one should introduce the angular correlation between $\vec{\lambda}$ and $\vec{\rho}$ and define the three-body densities.

$$h_{\sigma}^{(\rho)}(\rho, \lambda, \theta) = \int |P_{\sigma} \Psi(\vec{\rho}, \vec{\lambda})|^2 \rho^2 d\Omega_{\rho} \lambda \sin\theta d\phi_{\rho\lambda} \quad (12)$$

$$\text{normalized to} \quad \int h_{\sigma}^{(\rho)}(\rho, \lambda, \theta) \lambda d\lambda d\theta = g_{\sigma}(\rho) \quad (12')$$

$$\text{and} \quad h_{\sigma}^{(\lambda)}(\rho, \lambda, \theta) = \int |P_{\sigma} \Psi(\vec{\rho}, \vec{\lambda})|^2 \lambda^2 d\Omega_{\lambda} \rho \sin\theta d\phi_{\rho\lambda} \quad (13)$$

$$\text{normalized to} \quad \int h_{\sigma}^{(\lambda)}(\rho, \lambda, \theta) \rho d\rho d\theta = f_{\sigma}(\lambda) \quad (13')$$

which are simply related by

$$\lambda h_{\sigma}^{(\rho)}(\rho, \lambda, \theta) = \rho h_{\sigma}^{(\lambda)}(\rho, \lambda, \theta) \quad (14)$$

Here θ denotes the angle between $\vec{\lambda}$ and $\vec{\rho}$, and the integration measures have been chosen in order that $h_{\sigma}^{(\rho)}$ and $h_{\sigma}^{(\lambda)}$ are normalized as superficial densities with polar coordinates (ρ, θ) or (λ, θ) . Up to some factors, the density h is the square wave-function after that some trivial azimuthal symmetries have been removed or integrated out. Slices of the distributions $h(\rho, \lambda, \theta)$ at fixed ρ or at fixed λ provide sets of planar densities which allow one for a systematic hunting of diquark clustering.

III The proton trajectory (duu)

1 The ground state $L = 0$

We first analyze the case of the proton. The quark-diquark approximation described in section (II,2) is applied either for a vector diquark $(uu)_1$ or a scalar diquark $(ud)_0$. The comparison of the energies is presented in Table 1. With central forces only, the diquarks $(uu)_1$ or $(ud)_0$ are identical, and for the various types of potentials considered here, the quark-diquark approximation is rather poor (15%), the approximate mass being lower than the exact one. When spin forces are included, the scalar diquark $(ud)_0$ is lighter and more closely clustered, but this does not improve the quark-diquark approximation. Let us remark that the Pauli principle is correctly taken into account for $(uu)_1$ diquark, whereas, in the case of a $(ud)_0$ diquark, one neglects the antisymmetrisation of the two u's inside the proton. Indeed, in the standard three-quark wave-function of the proton, any (ud) pair is only 3/4 of the time in a spin singlet state.

We now examine the proton wave-function, defined first as a d -(uu) configuration, for which the Jacobi variable $\vec{\rho} \propto \vec{r}_2 - \vec{r}_3$ is the distance between the two u-quarks. The spin of the (uu) pair is $\sigma = 1$. The density distributions $g_{\sigma}(\rho)$ and $f_{\sigma}(\lambda)$, shown in Fig. 2, reach their maxima at similar values $R = 0.66$ fm and $D = 0.50$ fm, respectively, so that no striking evidence for a (uu) diquark is seen. In the upper part of Fig. 3, we plot slices of the three-body densities $h_1^{(\rho)}(R, \lambda, \theta)$ and $h_1^{(\lambda)}(\rho, D, \theta)$. In each case, one of the relative distance ρ and λ has been frozen to its most probable value. From this figure, there is no indication for a (ud) or (uu) type of diquark.

This conclusion is confirmed in a complementary analysis, where the proton is studied as a u -(du) configuration, with the Jacobi variable ρ attached to the d - u relative motion. As seen in the lower part of Fig. 3, where the $h_0^{(\rho)}(R, \lambda, \theta)$ and $h_0^{(\lambda)}(\rho, D, \theta)$ relative to a (ud) diquark coupling are plotted, all interquark distances have comparable mean values in the proton wave-function resulting from our single non-relativistic model.

2 The $L = 8$ excited state

The d -(uu)₁ and u -(ud)₀ quark-diquark approximations are now applied with the angular momentum $L = \hbar = 8$ carried by the relative motion of the quark and the diquark. The results are presented in Table 2 for linear and Bhaduri's potential. With central force only, the quark-diquark approximation is good up to 4%, being slightly better for Bhaduri's potential. When spin forces are added, the approximation remains good in both cases but the d -(uu) case seems better.

Let us now look at the wave-function. The one-variable densities $g_{\sigma}(\rho)$ and $f_{\sigma}(\lambda)$ do not give many information in the d -(uu)₁ channel, since $R = 2.44$ fm and $D = 1.36$ fm. As expected for an orbitally excited state, the system has a large spatial extension, but no diquark is seen so far. If we now turn to the u -(ud) configuration, the densities $g_{\sigma}(\rho)$ and $f_{\sigma}(\lambda)$ reach their maximum at $R = 0.92$ fm and $D = 2.28$ fm, respectively, indicating a (ud) diquark structure. This is confirmed

clearly by the various extracts of the three-body density $h(\rho, \lambda, \theta)$ displayed in Fig. 4. This leads to two comments :

i) Checking the validity of the quark-diquark approximation for the binding energy does not provide a very accurate test of the diquark structure. In the present example, it would favour $d\text{-(uu)}_1$ against $u\text{-(ud)}_0$

ii) Why is the $(ud)_0$ diquark favoured in this specific calculation? There are, in fact, two conflicting effects. First, the $(ud)_0$ diquark is lighter than the $(uu)_1$, as consequence of the chromomagnetic potential (3-4), and this favours the $(ud)_0\text{-u}$ configuration with respect to $(uu)_1\text{-d}$. On the other hand, the $(uu)_1\text{-d}$ binary system has a larger reduced mass and thus experiences less kinetic energy when l is increased. In the present calculation, the first effect is still slightly dominant for $l = 8$, but the state of $(ud)_0\text{-u}$ structure is only 95 MeV below the $(uu)_1\text{-d}$ one. As $l \rightarrow \infty$, the $(uu)_1\text{-d}$ state would be the lowest one. In the real world, relativistic effects, spin-orbit forces, coupling to decay channels, etc... would greatly influence the ordering of these states.

IV The Qqq systems

We now study the influence of mass asymmetry by considering single flavoured Λ or Σ baryons with strangeness, charm or beauty. As in the previous case, the $L=0$ and $L=8$ states are discussed separately.

1 The ground state $L = 0$

In Table 3 are displayed the results for the two possible diquark approximations, $Q\text{-(qq)}$ and $(Qq)\text{-q}$, using various potentials. The coulomb-plus-linear potential (1), the pure linear and the power-law (2) ones give roughly the same conclusions. The quark-diquark approximations are antivariational; the $Q\text{-(qq)}$ approximation corresponds to 10-15% deviation from the exact three-body energy while the $(Qq)\text{-q}$ one is much better at around 4-6% deviation. So we note a clear correlation between the diquark radius and the accuracy of the quark-diquark approximation : as expected, the smaller (Qq) diquark gives a better result than the (qq) one.

When spin effects are included, the difference between the $Q\text{-(qq)}$ and $(Qq)\text{-q}$ approximations is enlarged and the later is clearly favoured. Also the Λ baryons are much better reproduced than the Σ one. In summary, the accuracy of the diquark approximation is around 12%, and cannot be considered as extremely good for the case of a (qq) diquark, while it is much better for the case of a (Qq) diquark.

The wave-function of the Σ (suu) is analyzed in Fig. 5, using either the $u\text{-u}$ or the $u\text{-s}$ distance as the Jacobi variable ρ . No diquark structure emerges. The size of the Σ is similar the proton one, and the interquark distances have all the same average value of around 0,5 fm. No diquark structure was seen in other systems like sdu , Quu or Qud , where Q is some heavy quark.

2 The $L = 8$ states

The quark-diquark approximation to the energy is shown in Table 4, for both $Q\text{-(qq)}$ and $(Qq)\text{-q}$ cases. We are in the embarrassing situation where the approximations, although incompatible, seem both rather good (around 5 %). In fact, the exact spectrum contains several nearly degenerate states, of $Q\text{-(qq)}$ or of $(Qq)\text{-q}$ type, each of those being approximated by a particular quark-diquark configuration.

We note a change with respect to the proton case, for which the $(du)\text{-u}$ state was slightly below the $(uu)\text{-d}$ one. Here the lowest state of the Σ type is found to be $(uu)\text{-s}$. The (us) diquark is

obviously more deeply bound than the $(uu)_1$, but this is overcome by the fact that the $(uu)_1$ -s system, having a larger reduced mass, acquires more easily orbital excitation than the $(us)_0$ -u one. This tendency is even more pronounced for the cuu or buu cases. In figure 6 are shown the quark distribution densities for the lowest Σ state. The four pictures exhibit clearly a diquark structure of type (uu) -s.

V The qQQ systems

1 The ground state $L = 0$

In Table 5, the various quark-diquark approximations are displayed. The quality of the results is the same for the different types of potential. Clearly, the (QQ) approximation is much closer than the (qQ) one to the exact result, and the bigger is the ratio m_Q/m_q , the better is the accuracy (7% for uss , 1% for ucc). When spin effects are added, the quality deteriorates but, if the masses are sufficiently heavy, the QQ diquark approximation give again very good results.

The three systems uss , ucc and ubb were studied in that case. When the mass ratio m_Q/m_q is not very large, there is no marked diquark structure; however when this ratio is increased, a QQ diquark structure becomes more and more apparent. We illustrate this point on the ubb system in Fig. 7. In at least two of the four pictures, the QQ diquark is clearly signed. The natural tendency of the heavy particles to cluster each other is enforced by the attractive coulomb part of the potential, whereas the repulsive spin effects are very weak, since proportional to m_Q^{-2} .

2 The $L = 8$ states

The corresponding results are presented on Table 6. The diquark approximation of type QQ does not work at all ($\sim 15\%$ accuracy) and always give a mass larger than the exact one. On the other hand, the (qQ) diquark approximation is much better ($\sim 2\%$ accuracy) and is always antivariational.

The examination of the wave-function is very interesting. We present here the uss system but the conclusions are essentially the same for ucc . Fig. 8 corresponds neither to an isotropic configuration nor to a clear diquark structure. The state looks in fact like a QQ binary system, with a diluted q cloud in between. One can easily understand that one would never minimize the centrifugal energy $\frac{L(L+1)}{\mu R^2}$ with a (QQ)-q structure whose reduced mass is very light. The angular

momentum is almost entirely carried by the relative motion of the two heavy quarks, i.e. $l_p = 8$, whereas the light quark evolves in a s-wave state ($l_q = 0$), around the centre-of-mass of two heavy quarks. One should probably need very high L to have a (Qq) diquark showing up.

3. The Born-Oppenheimer approximation for qQQ

We have just seen that, while a q-(QQ) quark-diquark approximation is acceptable for $L = 0$, introducing angular momentum tends to separate the two heavy quarks without producing too much (qQ) clustering. In fact, the dynamics of the (qqQ) baryons is not well described in terms of diquarks. Instead, the Born-Oppenheimer method gives extremely convincing results.

For a fixed QQ separation p , one solves the one-body problem for the quark q, which is submitted to non-central forces. Relativistic variants are even allowed, using for instance bag models. The binding energy $E_0(p)$ of the quark, when added to the direct QQ interaction $V_{23}(p)$, gives an effective two-body potential $V_{QQ}(p)$, leading to a very accurate approximation of the first QQq energies and eigen wave-functions. Higher states correspond to second or higher adiabatics

$E_n(\rho)$, $n > 0$. As in many fields of physics, the Born-Oppenheimer method works much better than one would a priori expect. This is illustrated in Table 7. More details will be given elsewhere⁹.

VI Conclusions

In this paper we have performed some non-relativistic three-body calculations for various combinations of quark flavours, to examine to which extent baryons can be approximately described as a localized diquark surrounded by a quark. The comparison of the masses obtained in the quark-diquark approximation with the exact three-body calculation does not always provide unambiguous indications. Sometimes, a q_1 -(q_2q_3) mass computed in the quark-diquark approximation coincides accidentally with the lowest ($q_1q_2q_3$) system, whose structure is mostly (q_1q_2)- q_3 .

Our conclusion concerning the diquark clustering in our single non-relativistic models are essentially based on a systematic study of quark correlations in the three-body wave-function. There are only two cases where a diquark structure emerge clearly :

- i) In qQQ baryons with low angular momentum. The two Q quarks cluster under the combined effect of their heavyness, the attractive coulomb potential and the m_Q^{-2} suppression to the chromomagnetic repulsion.
- ii) In qqq or Qqq baryons with high angular momentum. In that case the centrifugal force which separates a single quark from a pair is the main ingredient. However, the type of diquark result from a subtle balance between the asymmetry which favours a qq diquark, and the spin-spin interaction allied to the Pauli principle, which favours a qQ diquark.

For $m_Q/m_q \gg 1$ a qq diquark will emerge, whereas for $m_Q/m_q \approx 1$ a qQ diquark occurs.

For other systems, either the quark density is rather isotropic (low angular momentum qqq systems) or the resulting structure is of a molecular type (qQQ with high angular momentum).

The arguments explaining diquark formation are "classical" in essence (for this we agree with ref 5), however, quantum effects cannot be ignored, especially the Pauli principle which forbids some configuration minimizing the classical hamiltonian.

Acknowledgments

We are particularly indebted to Pr. C. Gignoux for many illuminating discussions and constant interest in this work. Advices and encouragement of A. Martin, P. Kroll and E. Leader are gratefully acknowledged. We are very indebted to P. Olivero for valuable help concerning the graphical codes and to the CCPN for providing us computer facilities. We also thank J. Larruat for the realization of the photos.

References :

- 1 M. Gell-Mann, Phys. Lett. **8**, 214 (1964)
- 2 See e.g., B. Nicolescu and V. Poenaru, in "A passion for physics", Proceedings of the G.F. Chew Jubilee, Sept. 29, 1984, World Scientific Company, 1985; ed. by C. Detar, J. Finkelstein and C.I. Tan, pp 195-221
- 3 D.B. Lichtenberg, W. Namgung, E. Predazzi, J.G. Wills, Phys. Rev. Lett. **48**, 1653 (1982)
K.F. Liu, C.W. Wong, Phys. Rev. **D28**, 413 (1985)
- 4 J.L. Basdevant, S. Boukraa, Z. Phys **C28**, 413 (1985)
- 5 A. Martin Z. Phys **C32**, 359 (1985)
- 6 M. Fabre de la Ripelle, Few Body System suppl 2, Springer-Verlag (1987) pp 469-482 and pp 493-497
- 7 S. Fleck, B. Silvestre-Brac, C. Gignoux, J.M. Richard, in "The elementary Structure of Matter", Les Houches, France, 1987, ed. J.M. Richard et al, Springer Verlag (1988)
- 8 B. Silvestre-Brac, Talk given at the 9th session d'études biennale de Physique Nucléaire, Aussois, France, 1987
- 9 S. Fleck, Thèse de l'Université de Grenoble I.
- 10 see, e.g., W. Kwong, J.L. Rosner, C. Quigg, Ann. Rev. Nuc. Part. Sc. **37**, 1987, 325
- 11 A. Martin, Phys. Lett. **100B**, 511 (1981)
- 12 J.M. Richard, P. Taxil, Phys. Lett. **128B**, 453 (1983); Ann. Phys. (NY) **150**, 267 (1983)
- 13 R.K. Bhaduri, L.E. Cohler, Y. Nogami, Nuov. Cim. **60A**, 376 (1981)
- 14 S. Ono, F. Schöberl, Phys. Lett **188B**, 419 (1982)
- 15 B. Silvestre-Brac, C. Gignoux, Phys. Rev. **D32** 743 (1985)

Table 1

Potential	Exact			Diquark	
	$\sqrt{\langle r_{23}^2 \rangle}$	$\sqrt{\langle r_{12}^2 \rangle}$	E_{exact}	$q_1(q_2q_3)$	$(q_1q_2)q_3$
Marin	5,078	5,078	1,086	0,907	0,907
Linear	4,725	4,725	2,818	2,634	2,635
Bhaduri central	4,439	4,333	1,204	1,023	1,024
central + $\sigma.\sigma$	4,348	4,032	1,032	0,740	0,912

Table 2

	E_{exact}	$q_1(q_2q_3)$	$(q_1q_2)q_3$
Linear	5,315	5,052	5,058
Bhaduri central	3,843	3,703	3,709
central + $\sigma.\sigma$	3,771	3,722	3,638

Table 3

Potential		exact			diquark	
		$\sqrt{\langle r_{23}^2 \rangle}$	$\sqrt{\langle r_{12}^2 \rangle}$	E_{exact}	$q(q,q)$	$(q,q)q_3$
Martin	suu	4,934	4,481	1,268	1,321	1,234
	cuu	4,788	3,983	2,452	2,152	2,308
Linear	suu	4,688	4,362	2,983	2,772	2,835
	cuu	4,641	3,963	4,146	3,887	4,024
Bhaduri central	suu	4,378	4,057	1,354	1,141	1,203
	cuu	4,302	3,642	2,496	2,225	2,352
Bhaduri + spin-spin	suu	4,365	3,838	1,264	0,952	1,128
	sud	3,859	3,863	1,186	1,037	1,129
	cuu	4,391	3,608	2,493	2,155	2,323
	cud	3,440	3,790	2,327	2,136	2,324

Table 4

		E_{exact}	$q_1(q_2q_3)$	$(q_1q_2)q_3$
Linear	suu	5,213	4,868	5,235
	cuu	6,077	5,582	6,361
Bhaduri central	suu	3,735	3,554	3,841
	cuu	4,592	4,340	4,887
central + spin-spin	suu	3,754	3,569	3,783
	sud	3,667	3,502	3,785
	cuu	4,609	4,348	4,859
	cud	4,531	4,318	4,862

Table 5

		exact			diquark	
Potential		$\sqrt{\langle r_{23}^{-2} \rangle}$	$\sqrt{\langle r_{12}^{-2} \rangle}$	E_{exact}	$q(q_2q_3)$	$(q_1q_2)q_3$
Martin	ucc	2,326	3,673	3,685	3,634	3,396
	uss	3,782	4,338	1,430	1,321	1,234
Linear	ucc	2,756	3,847	5,409	5,357	5,237
	uss	3,937	4,322	3,141	3,025	2,969
Bhaduri central	ucc	2,345	3,458	3,686	3,629	3,424
	uss	3,612	3,995	1,493	1,375	1,311
central + $\sigma\sigma$	ucc	2,324	3,337	3,636	3,558	3,397
	uss	3,543	3,711	1,373	1,173	1,239

Table 6

		E_{exact}	$q_1(q_2q_3)$	$(q_1q_2)q_3$
Linear	uss	5,211	5,410	5,037
	ucc	6,854	7,667	6,745
Bhaduri central	uss	3,728	3,985	3,669
	ucc	5,340	6,129	5,285
central + $\sigma\sigma$	uss	3,694	3,997	3,618
	ucc	5,326	6,132	5,260

Table 7

	L=0	L=1	(L=0)*
Born-Oppenheimer	3,6840	3,9689	4,1092
Exact	3,6848	3,9712	4,1096

Figure Captions

Figure 1. Various geometries for quark distributions. R denotes the most probable interdistance between particles 2 and 3 while D is the most probable distance between particle 1 and the centre of mass of the pair (2-3). Case (1.a), $R < \sqrt{3} D$. Case (1.b) $R = D$, $\theta = \sqrt{3}\pi/2$. Case (1.c) $R = D$, $\theta = 0$ or π .

Figure 2. Two body density $g_{\sigma}(R_{23})$ (at the upper part) and one body density $f_{\sigma}(R_{1,23})$ (at the lower part) plotted versus the corresponding physical distances (in fm) for the proton system in its ground state. The u and u quarks are coupled either to spin $\sigma=0$ (dot-dashed line), to spin $\sigma=1$ (dotted line) or no matter the spin (full line).

Figure 3. Three body densities $h_{\sigma}^{(\rho)}(R, \lambda, \theta)$ (left-hand part) and $h_{\sigma}^{(\lambda)}(\rho, D, \theta)$ (right-hand part) calculated for the proton system $L = 0$ with Bhaduri's potential. In the upper part the particles 2 and 3 are the u quarks, while in the lower part, they are a u and a d quarks. The cross at the centre stands for the centre of mass of the pair (2-3) and the scale measured from the bottom left corner is 1 fm. The "fixed" particles are symbolized by a black circle, and their spin coupling by arrows. The various grey slices represent the spatial probabilities of finding the remaining particles.

Figure 4. Three body densities for the proton system in an orbital $L = 8$ excited state.

Figure 5. Three body densities for the Σ system suu in its ground state.

Figure 6. Three body densities for the Σ system suu in an orbital $L = 8$ excited state.

Figure 7. Three body densities for the ubb system in its ground state.

Figure 8. Three body densities for the Ξ system uss in an orbital $L = 8$ excited state.

Table Captions

- Table 1. Total mass (in GeV) for the proton ($q_1q_2q_3$) = (duu) system in its ground state obtained in a full three body calculation (exact) and with an approximation based on two types of diquarks (q_2q_3) and (q_1q_2). Two central potentials (Martin (2) and Bhaduri (1)) are tested and spin effects (4) are added in Bhaduri's potential. The mean square radii (in GeV^{-1}) are given also.
- Table 2. Same as in Table 1 for the proton (duu) system in an $L = 8$ orbital excited state. Only linear and Bhaduri's potential are tested.
- Table 3. Same as in Table 1 for two types of Qqq system : the $\Sigma = \text{suu}$ and the $\Sigma_c = \text{cuu}$.
- Table 4. Same as in Table 3 for the systems in an $L = 8$ orbital excited state.
- Table 5. Same as in Table 1 for two types of qQQ system : the $\Xi = \text{uss}$ and the ucc systems.
- Table 6. Same as in Table 6 for the system in an $L = 8$ orbital excited state.
- Table 7. Comparison of the binding energies calculated exactly or in the Born-Oppenheimer approximation for the (ccu) system with the central potential (2)

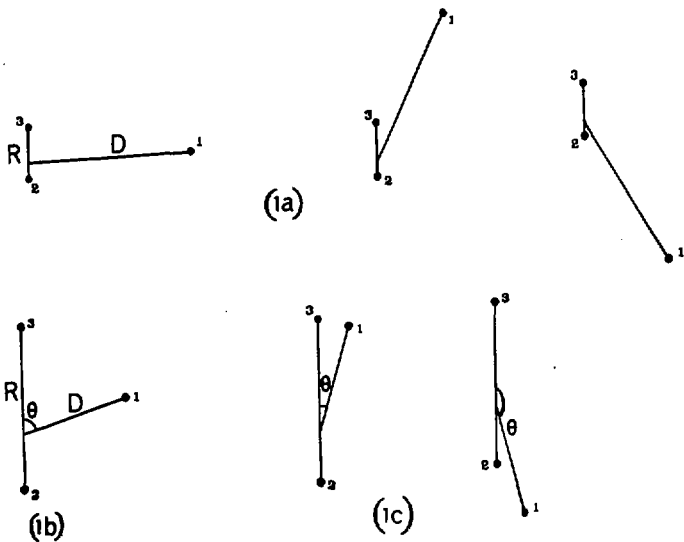
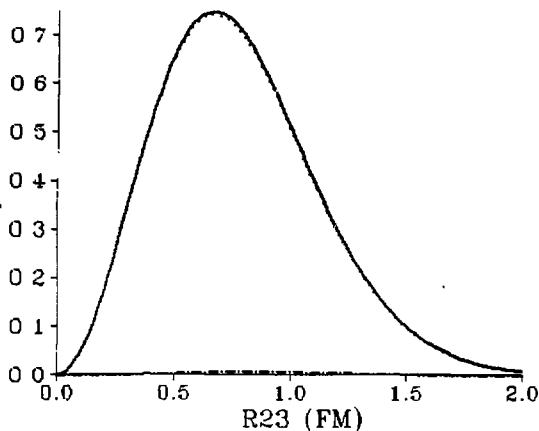


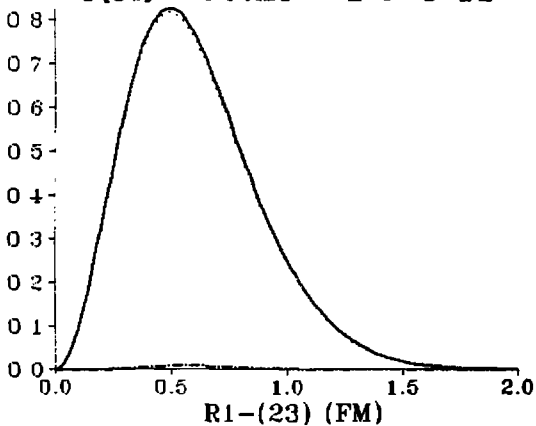
Figure 1

Figure 2

D(UU) POT:BD L=0 S=1/2



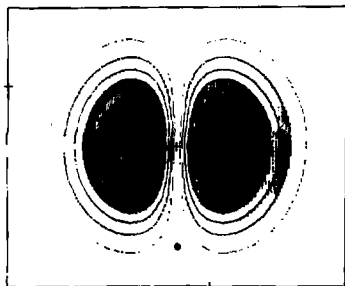
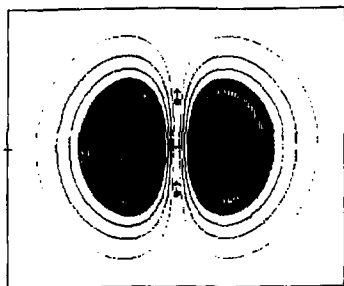
D(UU) POT:BD L=0 S=1/2



DUU)

POT:BD

$L=0$ $S=1/2$



U(UD)

POT:BD

$L=0$

$S=1/2$

$S_{23}=0$

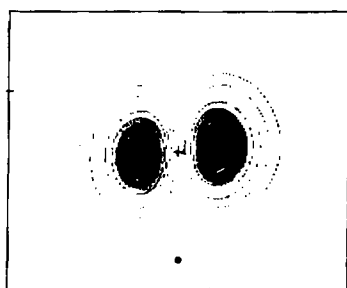
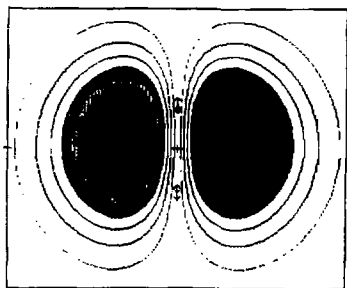
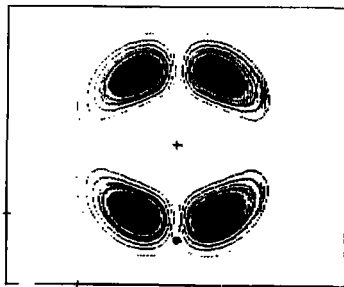
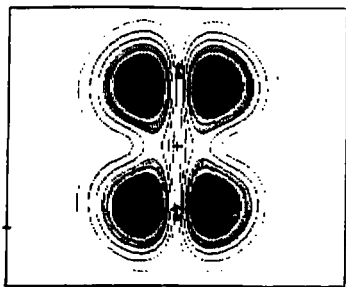


Fig 3

D(UU) POT:BD L=8 S=1/2 S₂₃=1



U(UD) POT:BD L=8 S=1/2 S₂₃=0

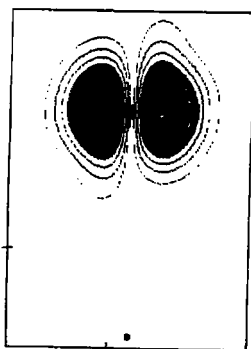
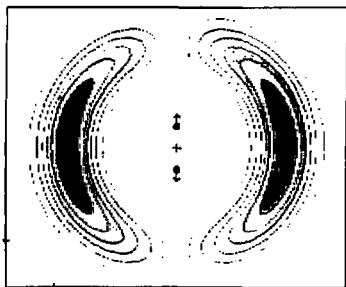


Figure 4

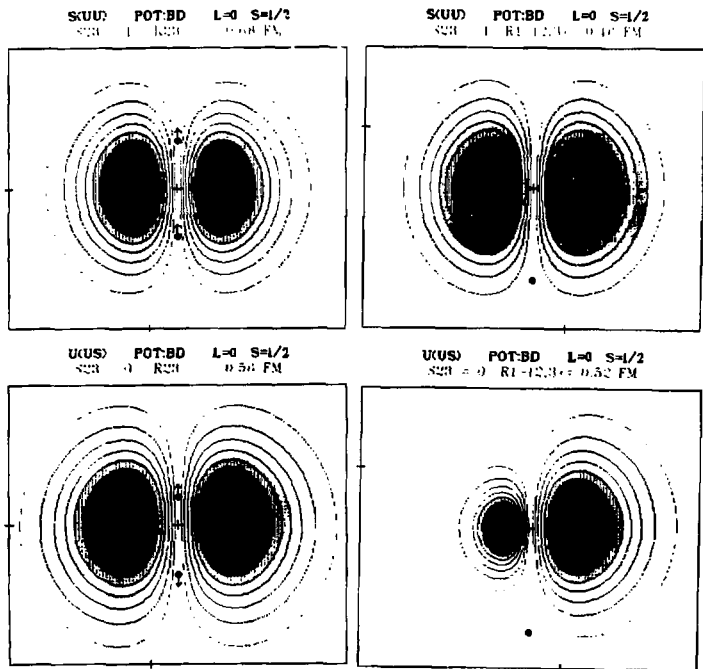


Figure 5

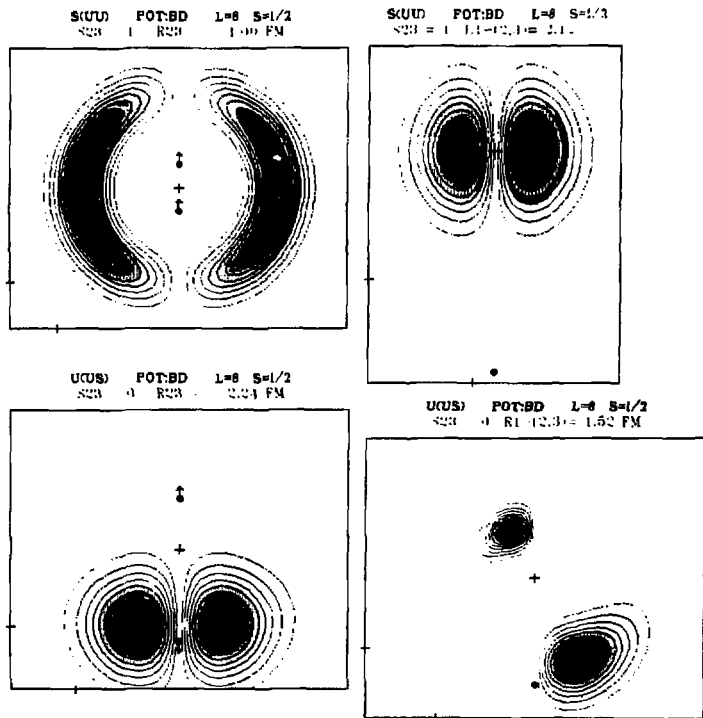
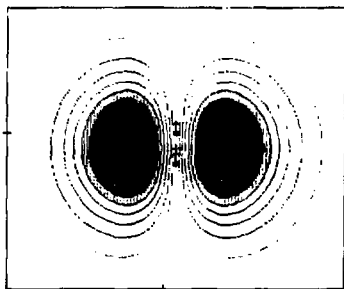
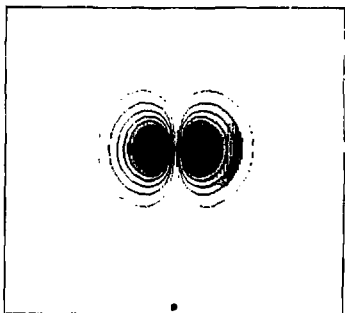


Figure 6

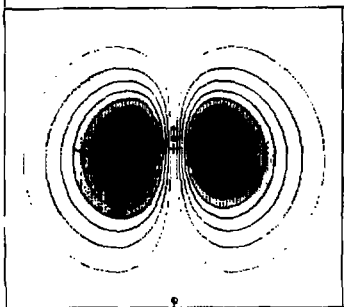
U(BB) POT:BD L=0 S=1/2
SQR 1 R23 0 16 FM



U(BB) POT:BD L=0 S=1/2
SQR 1 R1 10.0 0.07 FM



B(CUB) POT:BD L=0 S=1/2
SQR 0 R23 0 16 FM



B(CUB) POT:BD L=0 S=1/2
SQR 0 R1 10.0 0.20 FM

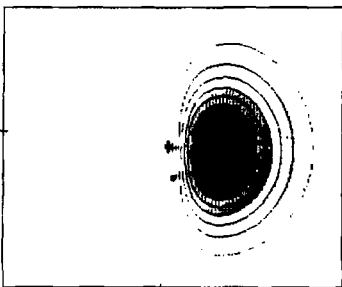


Figure 7

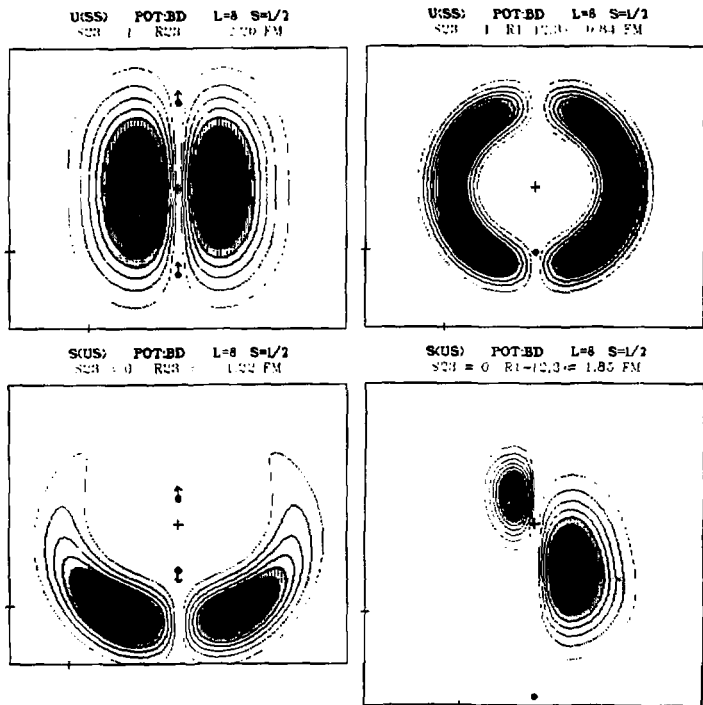


Figure 8